

## Oligo-Asp Tag/Zn(II) Complex Probe as a New Pair for Labeling and Fluorescence Imaging of Proteins

Akio Ojida, Kei Honda, Daisuke Shinmi, Shigeki Kiyonaka, Yasuo Mori, and Itaru Hamachi\*

Contribution from the Department of Synthetic Chemistry and Biological Chemistry, Graduate School of Engineering, Kyoto University, Katsura Campus, Nishikyo-ku, Kyoto, 615-8510, Japan

Received March 18, 2006; E-mail: ihamachi@sbchem.kyoto-u.ac.jp

**Abstract:** To accomplish the selective labeling of a specific protein in complicated biological systems, a peptide tag incorporated into the protein and a complementary small molecular probe are required. Although a variety of peptide tag/probe pairs have been developed as molecular tools for protein analyses, the availability of pairs suitable for real-time imaging of proteins is still limited. We now report a new peptide tag/artificial probe pair composed of a genetically encodable oligo-aspartate sequence (D4 tag, (D4)<sub>n</sub>, *n* = 1–3) and the corresponding multinuclear Zn(II) complexes (Zn(II)–DpaTyr). The strong binding affinity of the Zn(II)–DpaTyr probes with the D4 tag was a result of the multiple coordination bonds and the multivalent effect. It was measured quantitatively by isothermal titration calorimetry. The high affinity between the tag and the probe, indispensable for the selective protein labeling, enabled the pair to be used for the labeling and fluorescence imaging of a membrane-bound receptor protein tethering a triply repeated D4 tag ((D4)<sub>3</sub>) in an intact cell configuration without significantly affecting the receptor signal transduction.

### Introduction

A pair of a peptide tag incorporated into a protein and a complementary small molecular probe is now regarded as an indispensable analytical tool for a wide variety of biological studies. Some useful peptide tag/probe pairs, such as His tag with Ni(II)–NTA (nitrilotriacetic acid) and FLAG with the corresponding antibody, have been developed and are widely used for protein isolation using affinity column chromatography, protein/peptide immobilization on a microtiter plate, and sensitive protein detection using Western blotting.<sup>1</sup> In recent years, new types of peptide tag/small-molecule fluorescent probe pairs have been developed as valuable molecular tools for real-time imaging of target proteins in living cells.<sup>2</sup> Pioneering work was reported by Tsien and co-workers, describing a tetracysteine motif (–Cys–Cys–X–X–Cys–Cys–)/bisarsenical ligand (FlAsH) pair, the usefulness of which has been demonstrated in a number of bio-imaging experiments in living cells.<sup>2e,f</sup> Subsequently, Vogel et al. applied the conventional His tag (–(His)<sub>n</sub>–)/Ni(II)–NTA pair for fluorescence labeling of a protein on a cell surface.<sup>2h</sup> In contrast to the protein labeling techniques using green fluorescent proteins (GFPs) as a genetic fusion,<sup>3</sup> antibod-

ies, and quantum dots (QDs),<sup>4</sup> labeling with such a tag/small molecular probe pair is flexibly applicable for a wide variety of proteins with little or no interference with the function of the protein, because of its smaller size (GFPs, antibodies > 27 kDa, and QDs > 2–6 nm in diameter). Another intriguing feature of the tag labeling system is the interchangeability of the small molecular probe that enables the sequential labeling of proteins at different wavelengths (i.e., pulse-chase labeling). However, the availability of such a useful complementary pair is still limited, mainly due to the general difficulty in the design of the recognition pair with a high specificity. Thus, it would be highly desirable to develop a new pair in order to facilitate multiple labeling of distinct proteins in living systems, to allow flexibility for visualization of multiple proteins involved in complicated cellular events.

We now report a newly designed peptide tag/artificial probe pair that utilizes multivalent coordination chemistry between a genetically encodable oligo-aspartate sequence (D4 tag) and corresponding multinuclear Zn(II) complexes (Zn(II)–DpaTyr). This pair is orthogonal to the His tag/Ni(II)–NTA pair and applicable to the labeling and fluorescence imaging of the tag-fused proteins on a living cell surface as well as in a test tube (Figure 1).

### Results and Discussion

The metal–ligand interaction is potentially a versatile binding force for protein recognition since it can work effectively under physiological aqueous conditions.<sup>5</sup> Thus, the combination of a designed amino acid sequence and a metal complex might serve

(1) Terpe, K. *Appl. Microbiol. Biotechnol.* **2003**, *60*, 523.

(2) (a) Prescher, J. A.; Bertozzi, C. R. *Nat. Chem. Biol.* **2005**, *1*, 13. (b) Chen, I.; Ting, A. Y. *Curr. Opin. Biotechnol.* **2005**, *16*, 35. (c) Goldsmith, C. R.; Jaworski, J.; Sheng, M.; Lippard, S. J. *J. Am. Chem. Soc.* **2006**, *128*, 418. (d) Lata, S.; Gavutis, M.; Tampé, R.; Piehler, J. *J. Am. Chem. Soc.* **2006**, *128*, 2365. (e) Martin, B. R.; Giepmans, B. N. G.; Adams, S. R.; Tsien, R. Y.; *Nat. Biotechnol.* **2005**, *23*, 1308. (f) Gaietta, G.; Deerinck, T. J.; Adams, S. R.; Bouwer, J.; Tour, O.; Laird, D. W.; Sosinsky, G. E.; Tsien, R. Y.; Ellisman, M. H. *Science* **2002**, *296*, 503. (g) Howarth, M.; Takao, K.; Hayashi, Y.; Ting, A. Y. *Proc. Natl. Acad. Sci. U.S.A.* **2005**, *102*, 7583. (h) Guignet, E. G.; Hovius, R.; Vogel, H. *Nat. Biotechnol.* **2004**, *22*, 440.

(3) (a) Tsien, R. Y. *FEBS Lett.* **2005**, *579*, 927. (b) Miyawaki, A.; Sawano, A.; Kogure, T. *Nat. Cell. Biol.* **2003**, *5*, S1–S7.

(4) Green, M. *Angew. Chem., Int. Ed.* **2004**, *43*, 4129.

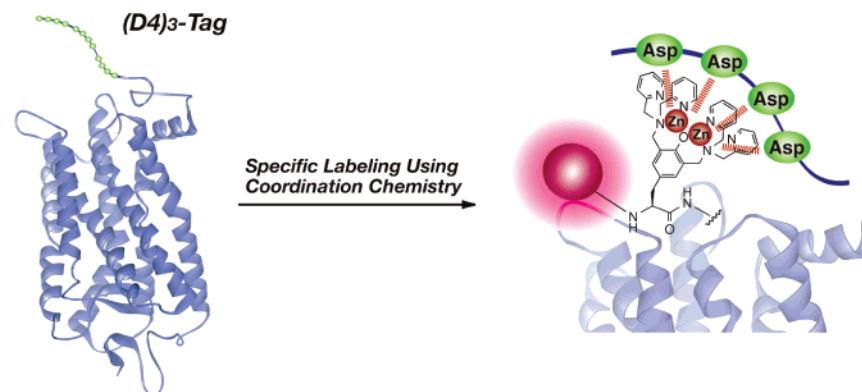


**Figure 1.** The new peptide tag/fluorescence probe pair for selective protein labeling reported herein.

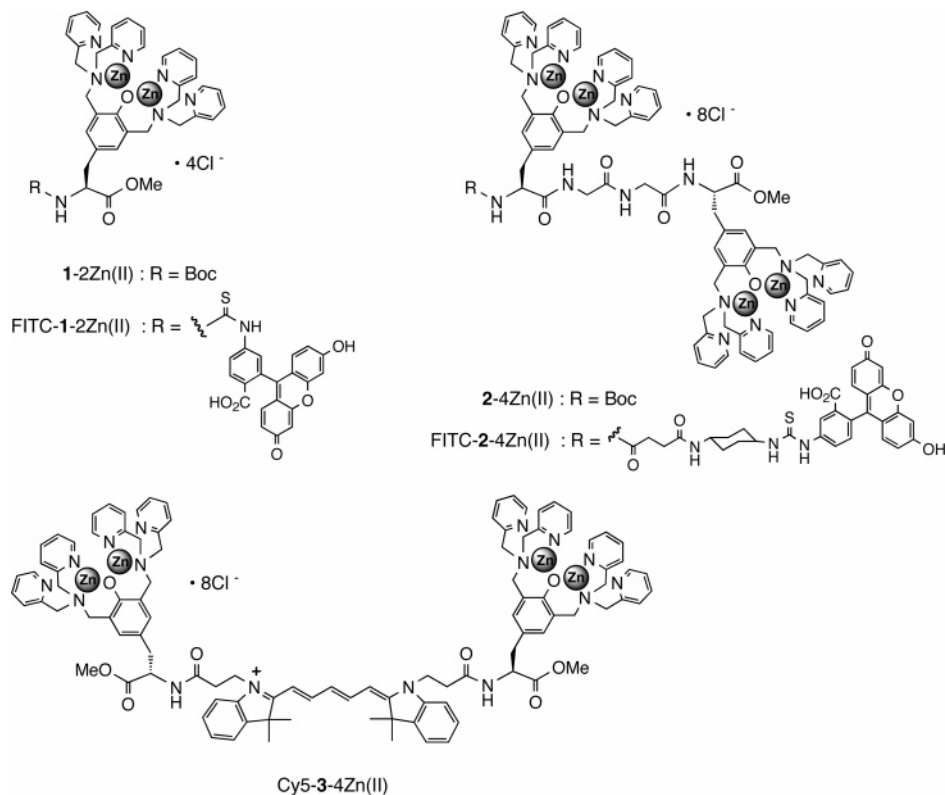


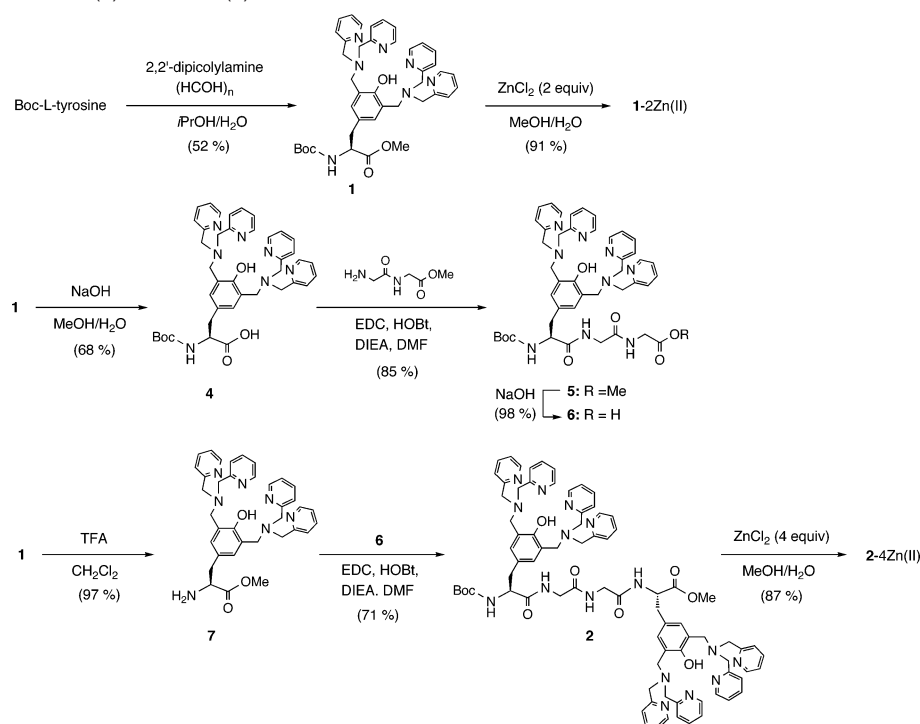
**Figure 2.** Molecular structures of the Zn(II)–DpaTyr and the fluorescent derivatives.

as a tag/artificial probe pair with a strong binding affinity suitable for selective labeling of the protein of interest. In this study, we designed a sequential oligo-aspartate as a short tag motif because of its accumulated carboxylate groups that favorably interact with a cationic metal complex, as well as its rare sequence among naturally occurring proteins.<sup>6</sup> It is anticipated that increasing the number of interactive amino acid residues should provide a stronger binding affinity and a higher selectivity, even by combining the same amino acid in a short tag sequence. Among a number of metal complexes, we selected the binuclear Zn(II)–Dpa (2,2′-dipicolylamine) complex based

on the L-tyrosine scaffold (Zn(II)–DpaTyr, Figure 2) for the following reasons: (1) the relative ease of synthesis and functionalization, which allows further structural modification and optimization, (2) the nonquenchable character of the d<sup>10</sup> transition metal Zn(II), necessary for the fluorescence probe, and (3) the preferable structural feature of the binuclear metal complex suitable for multipoint metal–ligand interactions. The syntheses of the binuclear 1-2Zn(II) and tetranuclear 2-4Zn(II) are shown in Scheme 1. The Mannich condensation of Boc-L-tyrosine with 2,2′-dipicolylamine and paraformaldehyde afforded the ligand **1**.<sup>7</sup> The dimeric ligand **2**, possessing Gly-Gly as a linker unit, was prepared from **1** by the standard condensation

(5) (a) Ojida, A.; Inoue, M.; Mito-oka, Y.; Tsutsumi, H.; Sada, K.; Hamachi, I. *J. Am. Chem. Soc.* **2006**, *128*, 2052. (b) Lata, S.; Reichel, A.; Brock, R.; Tampé, R.; Piehler, J. *J. Am. Chem. Soc.* **2005**, *127*, 10205. (c) Ojida, A.; Mito-oka, Y.; Sada, K.; Hamachi, I. *J. Am. Chem. Soc.* **2004**, *126*, 2454. (d) Ojida, A.; Inoue, M.; Mito-oka, Y.; Hamachi, I. *J. Am. Chem. Soc.* **2003**, *125*, 10184. (e) Ojida, A.; Mito-oka, Y.; Inoue, M.; Hamachi, I. *J. Am. Chem. Soc.* **2002**, *124*, 6256. (f) Fazal, M. A.; Roy, B. C.; Sun, S.; Mallik, S.; Rodgers, K. R. *J. Am. Chem. Soc.* **2001**, *123*, 6283. (g) Kapanidis, A. N.; Ebright, Y. W.; Ebright, R. H. *J. Am. Chem. Soc.* **2001**, *123*, 12123.

(6) A sequence analysis of human proteins in the Swiss-Prot Protein Knowledgebase revealed that the number of human proteins that possess an oligo-aspartate sequence (–DDDD–X<sub>n</sub>–DDDD–, where X is any amino acid and n = 0, 1, or 2) is 17. On the other hand, the number of human proteins that possess an oligo-glutamate sequence (–EEEE–X<sub>n</sub>–EEEE–, where X is any amino acid and n = 0, 1, or 2) is 158, which is much larger than that of the corresponding oligo-aspartate sequence. This is also an advantage of the oligo-aspartate tag.

**Scheme 1.** Synthesis of 1-2Zn(II) and 2-4Zn(II)

reactions. The complexation of both ligands with 2 and 4 equiv of  $\text{ZnCl}_2$  afforded the metal complexes **1-2Zn(II)** and **2-4Zn(II)**, respectively. We also prepared the fluorescein- or cyanine-labeled  $\text{Zn(II)}$ –DpaTyr derivatives as the corresponding fluorescent probes (FITC-**1-2Zn(II)**, FITC-**2-4Zn(II)**, and Cy5-**3-4Zn(II)**) by the stepwise condensation reactions and the subsequent  $\text{Zn(II)}$  complexations (Scheme 2). These probes were employed for the fluorescent imaging of the protein using fluorescence microscopy techniques. The detailed procedures for the syntheses of these  $\text{Zn(II)}$ –DpaTyr are described in the Supporting Information.

The binding affinity of **1-2Zn(II)** to the sequential oligo-aspartate motif was initially evaluated by isothermal titration calorimetry (ITC) experiments using the series of peptides D2–D5 (Boc- $\text{D}_n\text{-NH}_2$ ,  $n = 2\text{--}5$ , Table 1 and Figure 3a). The binding isotherms indicated that the binding process is exothermic and entropy-driven in all cases. The affinity becomes higher by almost 10-fold for a one-unit increase in Asp from D2 ( $(7.1 \pm 0.1) \times 10^3 \text{ M}^{-1}$ ), to D3 ( $(6.3 \pm 0.2) \times 10^4 \text{ M}^{-1}$ ), to the D4 peptide ( $(6.9 \pm 0.2) \times 10^5 \text{ M}^{-1}$ ). This trend seems to be saturated at the D4 peptide, since the binding affinity and the related thermodynamic parameters for D4 are almost comparable with those for D5. These data suggest that **1-2Zn(II)** can effectively interact with aspartate residues up to four units long in aqueous conditions.<sup>8,9</sup> To clarify the indispensability of the four aspartate units for the binding with **1-2Zn(II)**, ITC experiments with the alanine-substituted D4 peptides (Boc-

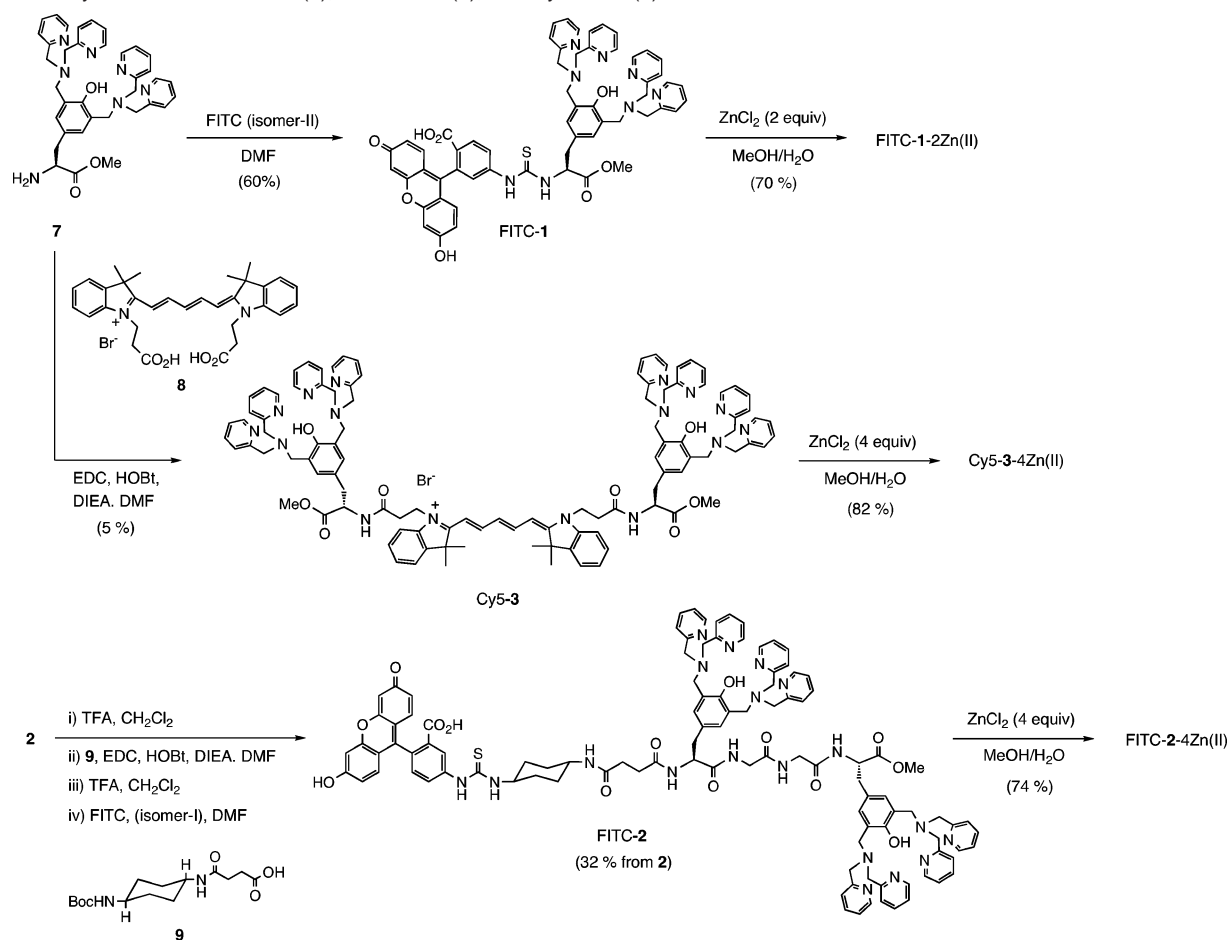
DADD- $\text{NH}_2$  and Boc-DAAD- $\text{NH}_2$ ) were also carried out (Table 1). The binding affinities with DADD and DAAD peptide were ca. 10-fold and 100-fold lower than that with D4, respectively, indicating that all four aspartate residues in D4 contribute to the binding with **1-2Zn(II)**. ITC experiments were also performed using the oligo-glutamate peptides (Boc- $\text{E}_n\text{-NH}_2$ ,  $n = 3$  or 4, Table 1). The results showed that the binding affinity of **1-2Zn(II)** with the E3 or E4 peptide is ca. 6-fold lower than that of D3 or D4 peptide, respectively, indicating that oligo-aspartate is better than oligo-glutamate. All these fundamental ITC experiments revealed that, among the tested model peptides, the aligned four aspartates (DDDD) is an optimal sequence for binding with  $\text{Zn(II)}$ –DpaTyr. Another interesting finding is that the interaction in both pairs of **1-2Zn(II)** and His6 peptide (H-YHHHHH- $\text{NH}_2$ ) and of  $\text{Ni(II)}$ –NTA and the D4 peptide was scarcely observed ( $K_{\text{app}} < 10^3 \text{ M}^{-1}$ , Table 2). The data suggest that the binding between D4 and **1-2Zn(II)** is orthogonal to the conventional His tag/ $\text{Ni(II)}$ –NTA binding.

The binding mode of **1-2Zn(II)** with the sequential  $\text{D}_n$  peptides was also evaluated by circular dichroism (CD) spectroscopy. A large induced CD (i-CD,  $\theta_{\text{max}} = 304 \text{ nm}$ ) in the UV absorption region of the  $\text{Zn(II)}$ –phenolate moiety of **1-2Zn(II)** was observed upon addition of D4, suggesting that a chiral environment was induced at the  $\text{Zn(II)}$  coordination sphere by the peptides (Figure 4a). The plot of the i-CD at 304 nm afforded a saturation curve (Figure 4a, insert), which was analyzed by a curve-fitting analysis to give a binding constant of  $1.4 \times 10^6 \text{ M}^{-1}$  for the D4 peptide, in agreement with that evaluated in the ITC experiment. The CD titration experiments with other peptides showed that increasing the number of aspartate residues

(7) Sun, L.; Burkitt, M.; Tamm, M.; Raymond, M. K.; Abrahamsson, M.; LeGourrière, D.; Frapart, Y.; Magnuson, A.; Kenéz, P. H.; Brandt, P.; Tran, A.; Hammarström, L.; Styring, S.; Åkermar, B. *J. Am. Chem. Soc.* **1999**, *121*, 6834.

(8) The binding between **1-2Zn(II)** (25  $\mu\text{M}$ ) and the D4 peptide was also evaluated by ITC under slightly acidic conditions (50 mM MES buffer, pH 5.5). Heat evolution due to the complex formation ceased sharply after the addition of 1.5 equiv of the D4 peptide. This suggests that the binding affinity of **1-2Zn(II)** for the D4 peptide is partially maintained under the acidic conditions, though detailed thermodynamic analysis cannot be done because the resultant binding isotherm is biphasic.

(9) In the ITC experiment of **1-2Zn(II)** (25  $\mu\text{M}$ ) with chondroitin sulfate (100  $\mu\text{g/mL}$ ) or sulfate anion (1 mM), no heat evolution due to complex formation was observed. In addition, the binding of **1-2Zn(II)** with the D4 peptide was completely retained, even in the presence of chondroitin sulfate (500  $\mu\text{g/mL}$ ), in the titration solution containing the D4 peptide (0.5 mM). These results indicate that the binding affinity of the  $\text{Zn(II)}$ –DpaTyr for the polysulfates on cell surface is sufficiently weak ( $< 10^3 \text{ M}^{-1}$ ).

**Scheme 2.** Synthesis of FITC-1-2Zn(II), FITC-2-4Zn(II), and Cy5-3-4Zn(II)**Table 1.** Stoichiometry ( $n$ ), Binding Constant ( $K_{\text{app}}$ ,  $\text{M}^{-1}$ ), Enthalpy ( $\Delta H$ ,  $\text{kcal mol}^{-1}$ ), and Entropy ( $T\Delta S$ ,  $\text{kcal mol}^{-1}$ ) for the Interactions of 1-2Zn(II) with the Oligo-aspartate<sup>a</sup> and Oligo-glutamate Peptides<sup>b,c</sup>

	1-2Zn(II)				1-2Zn(II)			
	D2	D3	D4	D5	DADD	DAAD	E3	E4
$n$	0.99	0.99	0.87	0.81	1.00	1.00	0.86	0.91
$K_{\text{app}}$	$(7.1 \pm 0.1) \times 10^3$	$(6.3 \pm 0.2) \times 10^4$	$(6.9 \pm 0.2) \times 10^5$	$(8.6 \pm 0.4) \times 10^5$	$(5.8 \pm 0.3) \times 10^4$	$(6.1 \pm 0.1) \times 10^3$	$(1.4 \pm 0.1) \times 10^4$	$(1.3 \pm 0.1) \times 10^5$
$\Delta H$	$-6.2 \pm 0.2$	$-5.2 \pm 0.1$	$-6.1 \pm 0.0$	$-6.5 \pm 0.2$	$-5.2 \pm 0.2$	$-5.9 \pm 0.2$	$-6.2 \pm 0.0$	$-7.2 \pm 0.1$
$T\Delta S$	-1.0	1.4	1.9	1.6	1.4	-0.76	-0.56	-0.24

<sup>a</sup>  $Dn = \text{Boc}-(\text{Asp})_n-\text{NH}_2$  ( $n = 2-5$ ), DADD =  $\text{Boc}-\text{Asp}-\text{Ala}-\text{Asp}-\text{Asp}-\text{NH}_2$ , DAAD =  $\text{Boc}-\text{Asp}-\text{Ala}-\text{Ala}-\text{Asp}-\text{NH}_2$ . <sup>b</sup>  $En = \text{Boc}-(\text{Glu})_n-\text{NH}_2$  ( $n = 3$  or  $4$ ). <sup>c</sup> Measurement conditions: 50 mM HEPES (pH 7.2), 25 °C.

from D2 to D4 afforded stronger binding in the interaction (Table S1), and the Job plot monitored by the CD titration between 1-2Zn(II) and D4 peptide clearly indicated that the binding stoichiometry is 1:1 (Figure 4b). These data also suggest that all four aspartate residues are essential for the tight binding with 1-2Zn(II).

The validity of the present D4 tag/Zn(II)–DpaTyr pair on a protein surface was evaluated using a soluble protein, mutant RNases, having a D4 (DDDD) or longer D4-G-D4 (DDDD-G-DDDD) peptide tag at the N-terminal. The binding affinity of 1-2Zn(II) or the dimeric 2-4Zn(II) for the mutant RNases was determined by the ITC experiments in aqueous conditions with a high ionic strength, i.e., 50 mM HEPES buffer (pH 7.2), 100 mM NaCl (Table 2, Figure 3b). The 1:1 binding stoichiometry ( $n = 1.0$  or  $0.93$  for 1-2Zn(II)/D4-RNase or 2-4Zn(II)/D4-G-D4-RNase, respectively) was confirmed by the binding isotherms in both cases. It should be noted that the moderate binding affinity for 1-2Zn(II) with D4-RNase ( $K_{\text{app}} = (1.2 \pm$

$0.2) \times 10^4 \text{ M}^{-1}$ ) is significantly enhanced by the polyvalent interaction possible with 2-4Zn(II), which had a 1000-fold stronger affinity ( $K_{\text{app}} = (1.8 \pm 0.3) \times 10^7 \text{ M}^{-1}$ ) for D4-G-D4-RNase. These results indicate that a strategy based on multivalent coordination chemistry on a protein surface achieves tight binding in aqueous solution.<sup>10</sup> No interference with the enzymatic activity of RNase by the tethered D4 tag was observed.<sup>11</sup> It is noteworthy that no significant interaction was observed in the ITC measurement ( $K_{\text{app}} < 10^3 \text{ M}^{-1}$ ) (Table 2) either between 2-4Zn(II) and a His tag (HHHHHH) appended RNase or between Ni(II)–NTA and a D4-RNase. These results again suggest that the D4 tag/probe pair is orthogonal to the

(10) (a) Mammen, M.; Choi, S.-K.; Whitesides, G. M. *Angew. Chem., Int. Ed.* **1998**, *37*, 2754. (b) Gestwicki, J. E.; Cairo, C. W.; Strong, L. E.; Oetjen, K. A.; Kiessling, L. L. *J. Am. Chem. Soc.* **2002**, *124*, 14922.

(11) The enzymatic activity of D4-RNase was evaluated by the initial rate of hydrolysis of polyuridylic acid as a substrate. The initial reaction rate was  $(2.63 \pm 0.04) \times 10^{-6} \text{ M} \cdot \text{min}^{-1}$ , almost identical with that of native RNase  $((2.92 \pm 0.02) \times 10^{-6} \text{ M} \cdot \text{min}^{-1})$ .



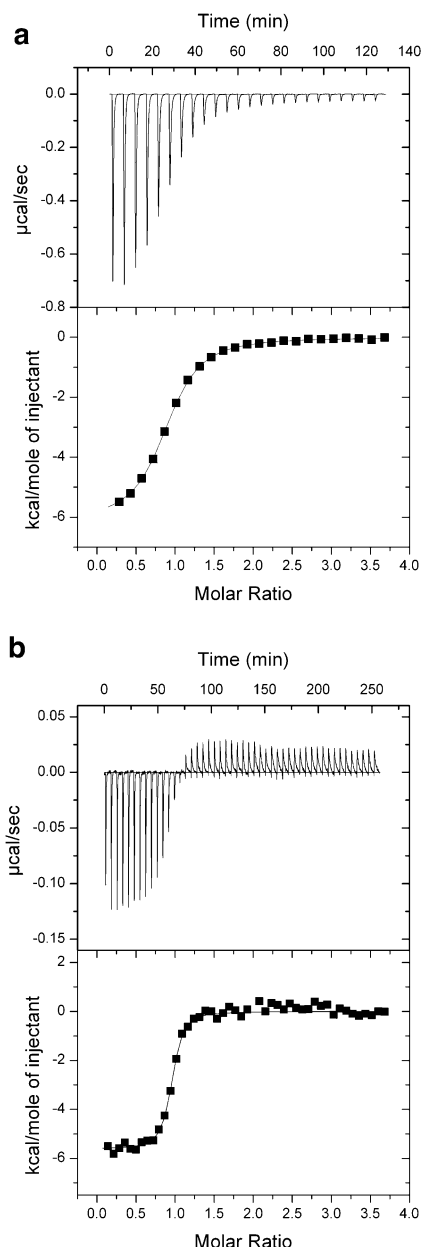


**Figure 3.** ITC titration curve (upper) and processed data (lower). (a) Titration of 1-2Zn(II) with the D4 peptide. Measurement conditions: [1-2Zn(II)] = 25  $\mu$ M, [D4] = 0.5 mM (10  $\mu$ L  $\times$  24 injections), 50 mM HEPES buffer, pH 7.2, 25  $^{\circ}$ C. (b) Titration of 2-4Zn(II) with D4-G-D4-RNase. Measurement conditions: [D4-G-D4-RNase] = 10  $\mu$ M, [2-4Zn(II)] = 0.2 mM (5  $\mu$ L  $\times$  48 injections), 50 mM HEPES buffer, pH 7.2, 100 mM NaCl, 25  $^{\circ}$ C.

conventional His tag/probe pair, and thus the two tag systems can be used simultaneously without affecting each other in biological studies.

To demonstrate the potential utility of the present tag/probe pair under biological conditions, we subsequently conducted the fluorescent labeling of a target protein on the surface of mammalian cells. The muscarinic acetylcholine receptor (mAChR) represents one of the most important G-protein-coupled receptors (GPCRs) and has been studied extensively with respect to fundamental biology and therapeutic application.<sup>12</sup> For the labeling experiment, a porcine m1-type AChR tethering a triply repeated D4 sequence (-DDDDG-  $\times$ 3) at the exoplasmic

N-terminus ((D4)<sub>3</sub>-m1AChR) was expressed in CHO cells. As the corresponding probes, the fluorescently modified Zn(II)-DpaTyr derivatives, FITC-1-2Zn(II), FITC-2-4Zn(II), and Cy5-3-4Zn(II), were used. During the initial stage of the labeling experiment, it was found that premixing the fluorescent probe with the D4 peptide (Boc-DDDD-NH<sub>2</sub>) was effective for suppressing the nonselective labeling of the cells, thereby enhancing the labeling specificity. Thus, after a short incubation (<10 min) of CHO cells expressing (D4)<sub>3</sub>-m1AChR with a 2  $\mu$ M concentration of FITC-2-4Zn(II) in the presence of a 20  $\mu$ M concentration of D4 peptide, a fluorescence image due to the FITC was observed on the cell surface by confocal laser scanning microscopy (Figure 5a). The fluorescence image became smeared by washing with a high concentration of inorganic pyrophosphate (100  $\mu$ M), a strong ligand for the Zn(II)-DpaTyr,<sup>13</sup> indicating the reversibility of the labeling technique as well as the significance of the coordination chemistry in the cell imaging (data not shown). On the other hand, no clear fluorescence images were obtained when the monomeric FITC-1-2Zn(II) was used, probably due to the lower binding affinity with (D4)<sub>3</sub>-m1AChR (data not shown). In addition, the fluorescence image with FITC-2-4Zn(II) was scarcely observed when wild-type CHO cells (data not shown) or CHO cells expressing m1AChR tethering a His tag instead of the D4 tag (Figure 5b) were used. To confirm that the fluorescence image originated from the labeled m1AChR located on the cell surface, the labeling experiment was carried out using receptor fused to the fluorescent EGFP ((D4)<sub>3</sub>-EGFP-m1AChR). After a short incubation (7 min) with Cy5-3-4Zn(II) in the presence of a 20  $\mu$ M concentration of the D4 peptide, fluorescence due to the Cy5 was detected on the cell surface (Figure 5d). This fluorescence image overlapped well with that of (D4)<sub>3</sub>-EGFP-m1AChR (Figure 5c,e), indicating the colocalization of the EGFP-fused m1AChR and Cy5-3-4Zn(II) on the cell membrane surface. A similar overlapping fluorescence image was detected in the labeling of DsRed-fused (D4)<sub>3</sub>-m1AChR with FITC-2-4Zn(II) (Figure S1, Supporting Information). The fluorescence intensity level of Cy5-3-4Zn(II) in cells transfected with the EGFP-fused m1AChR was significantly higher than that in wild-type CHO cells, as shown in Figure 5g, also supporting the selective labeling of the tagged m1AChR with Cy5-3-4Zn(II).<sup>14</sup> The cell toxicity of the labeling probe was assessed by comparing the growth rate of the CHO cells in the presence or absence of Zn(II)-DpaTyr (Figure S3). The treatment of the CHO cells with 1-2Zn(II) (10  $\mu$ M) and 2-4Zn(II) (1  $\mu$ M) for 15 min did not affect the cell growth rate within 24 h, indicating that Zn(II)-DpaTyrs do not exhibit significant toxicity and cell death induction.

To confirm whether the conjugate of the small D4 tag and the Zn(II)-DpaTyr probe exerts any influence on the m1AChR function, we measured the receptor-activated Ca<sup>2+</sup> signaling of the CHO cells. The intracellular Ca<sup>2+</sup> concentration ([Ca<sup>2+</sup>]<sub>i</sub>), which was monitored by the ratio of the fura-2 emission excited at 340 and 380 nm (ex<sub>340</sub>/ex<sub>380</sub>), increased upon the addition of carbachol, a potent agonist of m1AChR. The [Ca<sup>2+</sup>]<sub>i</sub> responses elicited by (D4)<sub>3</sub>-m1AChR were nearly identical to those elicited

(12) Felder, C. C. *FASEB J.* **1995**, *9*, 619.

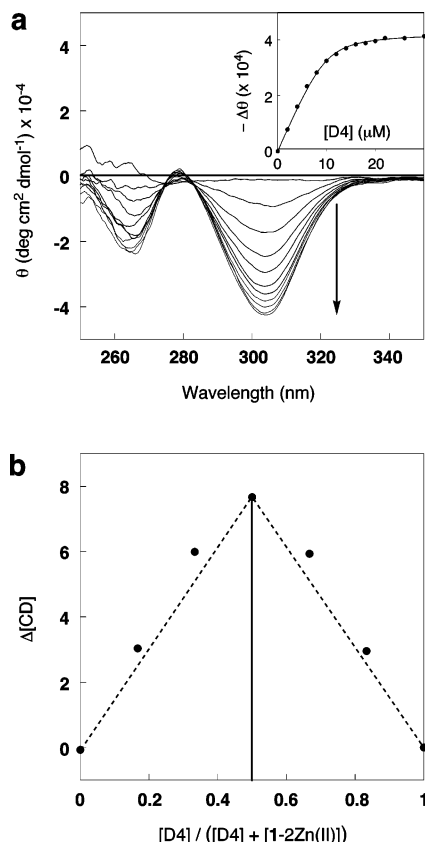
(13) Lee, D. H.; Im, J. H.; Son, S. U.; Chung, Y. K.; Hong, J.-I. *J. Am. Chem. Soc.* **2003**, *125*, 7752.

(14) The in vitro fluorescence titration experiment confirmed that the fluorescence intensity of Cy5-3-4Zn(II) scarcely changed upon binding to the D4-G-D4 peptide.

**Table 2.** Stoichiometry ( $n$ ), Binding Constant ( $K_{\text{app}}$ ,  $\text{M}^{-1}$ ), Enthalpy ( $\Delta H$ ,  $\text{kcal mol}^{-1}$ ), and Entropy ( $T\Delta S$ ,  $\text{kcal mol}^{-1}$ ) for the Interactions of the DpaTyr or Ni(II)–NTA with the Aspartate Peptides,<sup>a</sup> the His6 Peptide,<sup>b</sup> or the RNases Tethering a Tag<sup>c</sup>

	1-2Zn(II)			Ni(II)–NTA		2-4Zn(II)		
	His6 <sup>d</sup>	D4-RNase <sup>e</sup>	RNase <sup>e</sup>	D4 <sup>d</sup>	D4-RNase <sup>e</sup>	D4-G-D4-RNase <sup>e</sup>	His6-RNase <sup>e</sup>	RNase <sup>e</sup>
$n$	<10 <sup>3</sup>	1.00	<10 <sup>3</sup>	<10 <sup>3</sup>	<10 <sup>3</sup>	0.93	<10 <sup>3</sup>	<10 <sup>3</sup>
$K_{\text{app}}$		$(1.2 \pm 0.2) \times 10^4$				$(1.8 \pm 0.3) \times 10^7$		
$\Delta H$		$-1.2 \pm 0.4$				$-5.6 \pm 0.0$		
$T\Delta S$		4.4				4.3		

<sup>a</sup> D4 = Boc-(Asp)<sub>4</sub>-NH<sub>2</sub>. <sup>b</sup> His6 = H-YHHHHHH-NH<sub>2</sub>. <sup>c</sup> D4 (DDDD-) or D4-G-D4 (DDDD-G-DDDD-) or His (HHHHHH-) tag is attached to the N-terminal of the RNase. <sup>d</sup> Measurement conditions: 50 mM HEPES (pH 7.2), 25 °C. <sup>e</sup> Measurement conditions: 50 mM HEPES (pH 7.2), 100 mM NaCl, 25 °C.

**Figure 4.** Binding analysis of 1-2Zn(II) with the D4 peptide by circular dichroism (CD). (a) CD titration of 1-2Zn(II) (10  $\mu\text{M}$ ) with the D4 peptide;  $[\text{D4}] = 0\text{--}30\ \mu\text{M}$ . Inset) Plot of the  $\Delta\text{CD}$  value at 304 nm in the titration of 1-2Zn(II) with the D4 peptide. (b) CD Job plot between 1-2Zn(II) and the D4 peptide. The total concentration of both compounds is 40  $\mu\text{M}$ . Measurement conditions: 50 mM HEPES, pH 7.2, 25 °C.

by wt-m1AChR (Figure S2, Supporting Information). The effect of binding Zn(II)–DpaTyr on the activity of (D4)<sub>3</sub>-m1AChR was also evaluated. As shown in Figure 6a,b, the  $[\text{Ca}^{2+}]_i$  signaling stimulated by carbachol was not affected by the presence of FITC-2-4Zn(II) or Cy5-3-4Zn(II), indicating that these probes did not interfere with the original activity of (D4)<sub>3</sub>-m1AChR or the evoked intracellular signaling. The results of the cell labeling experiments demonstrated that the fluorescent probes comprising binuclear Zn(II)–DpaTyr selectively bind to the D4 motif tethered to the m1AChRs by multivalent coordination, so as to enable fluorescent labeling and imaging of m1AChR localization on the cell surface without interference with receptor function.

In conclusion, we successfully demonstrated that the D4 tag/Zn(II)–DpaTyr pair developed here is viable as a new molecular tool for protein labeling orthogonal to the His tag system. The

tag–probe interaction achieved by multiple coordination chemistry, as well as a multivalent effect, was sufficiently strong for the pair to be applied successfully to the fluorescence labeling and imaging of the receptor protein on the living cell surface. The rapid protein labeling, complete within 10 min by simple incubation, is a practical advantage in this labeling system. We envision further application of the D4 tag/Zn(II)–DpaTyr pair for protein labeling studies. With rapid advancements in enzyme-based labeling techniques, the methodology of selective protein labeling has attracted much attention in recent years.<sup>2g,15</sup> The tunable cell permeability of the Zn(II)–DpaTyr probes may offer the possibility of multiple labeling experiments with distinct proteins in living cells using a combination of enzyme-based or other tag/probe pair labeling methods.<sup>16</sup> However, a complication might conceivably arise due to the relatively large size of the dimeric Zn(II)–DpaTyr probes (ca. 2 kDa), which might interfere with the function of labeled protein in some cases. Further structural modification is desirable to downsize the labeling probe, to facilitate the utility of the present D4 tag system in bio-imaging studies. In addition, we envision that the present D4 tag/Zn(II)–DpaTyr pair could be used not only as a bio-imaging tool but also as a functional regulator of a specific protein using the chromophore-assisted light inactivation (CALI) technique,<sup>17</sup> or as a protein capture or immobilizing agent utilizing reversible noncovalent binding.

## Experimental Section

**General Methods.** Unless otherwise noted, all chemical reagents were purchased from commercial suppliers and used without further purification. <sup>1</sup>H NMR spectra were recorded using a JNM-EX400 (JEOL, 400 MHz) spectrometer, and the chemical shifts ( $\delta$ , ppm) are referenced to the respective solvent. FAB and MALDI-TOF mass spectra were recorded using QP5050A (Shimadzu) and Voyager DE-SP (PerSeptive Biosystems) instruments, respectively. Reverse-phase HPLC was conducted with a Lachrom (Hitachi) instrument with C18 columns.

**Synthesis of the Zn(II)–DpaTyr.** The Zn(II)–DpaTyr and their fluorescence derivatives were prepared according to the synthetic routes shown in Schemes 1 and 2. Detailed synthetic procedures and compound characterizations are described in the Supporting Information.

- (15) (a) Mercer, A. D.; Burkart, M. D. *Nat. Chem. Biol.* **2006**, *2*, 8. (b) Vivero-Pol, L.; George, N.; Krumm, H.; Johnsson, K.; Johnsson, N. *J. Am. Chem. Soc.* **2005**, *127*, 12770. (c) Yin, J.; Liu, F.; Li, X.; Walsh, C. T. *J. Am. Chem. Soc.* **2004**, *126*, 7754. (d) Keppler, A.; Gendrezig, S.; Gronemeyer, T.; Pick, H.; Vogel, H.; Johnsson, K. *Nat. Biotechnol.* **2003**, *21*, 86.
- (16) Since FITC-2-4Zn(II) and Cy5-3-4Zn(II) are not membrane-permeable, they are useful for the labeling of cell-surface membrane receptor. On the other hand, we found that the fluorescent DpaTyr dimers, having a BODIPY or a rhodamine derivative, can penetrate through the cell membrane so that these derivatives localize in the cytoplasm of CHO cell.
- (17) (a) Horskotte, E.; Schröder, T.; Niewöhner, J.; Thiel, E.; Jay, D. G.; Henning, S. W. *Photochem. Photobiol.* **2005**, *81*, 358. (b) Tour, O.; Meijer, R. M.; Zacharias, D. A.; Adams, S. R.; Tsien, R. Y. *Nat. Biotechnol.* **2003**, *21*, 1505.

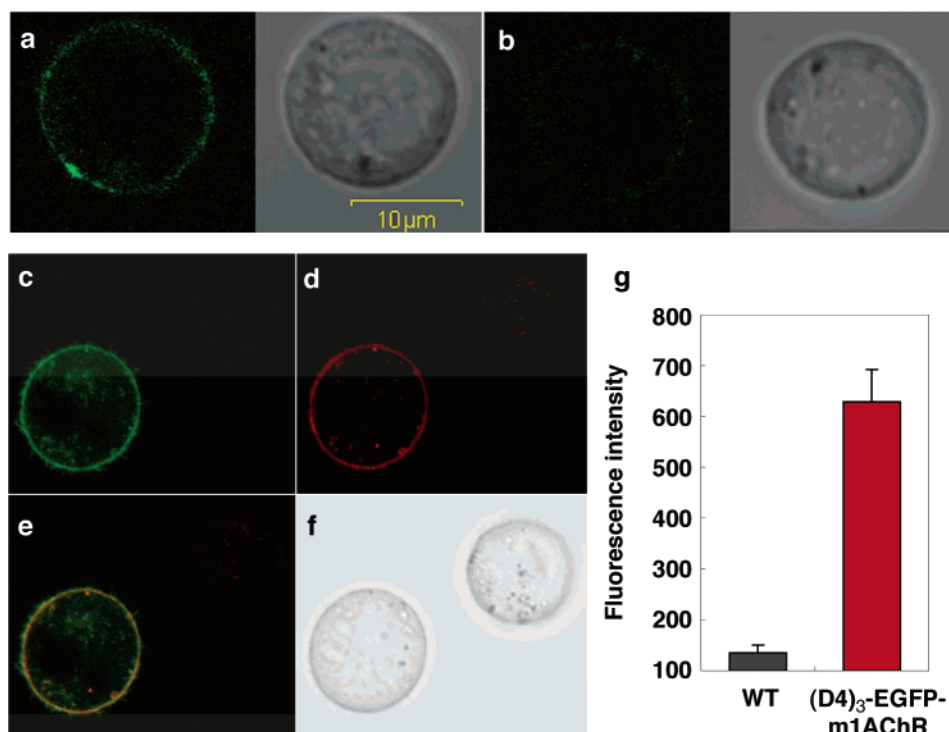


**Figure 5.** Labeling of muscarinic acetylcholine receptor (m1AChR) with the fluorescence label, Zn(II)-DpaTyr. (a,b) Fluorescent labeling of m1AChR tethering a D4 tag (D4  $\times$  3) (a) or His tag (b) with FITC-2-4Zn(II). The images on the right are transmission micrographs. (c–f) Fluorescent labeling of the (D4)<sub>3</sub>-EGFP-m1AChR with Cy5-3-4Zn(II). Cells were imaged simultaneously for EGFP (c) and Cy5-3-4Zn(II) (d). The overlay image of (c) and (d) is shown in (e); (f) is a transmission micrograph. (g) The average fluorescence intensity of Cy5-3-4Zn(II) in wild-type CHO cells (left) and CHO cells expressing (D4)<sub>3</sub>-EGFP-m1AChR (right) ( $N > 30$  in both cases).

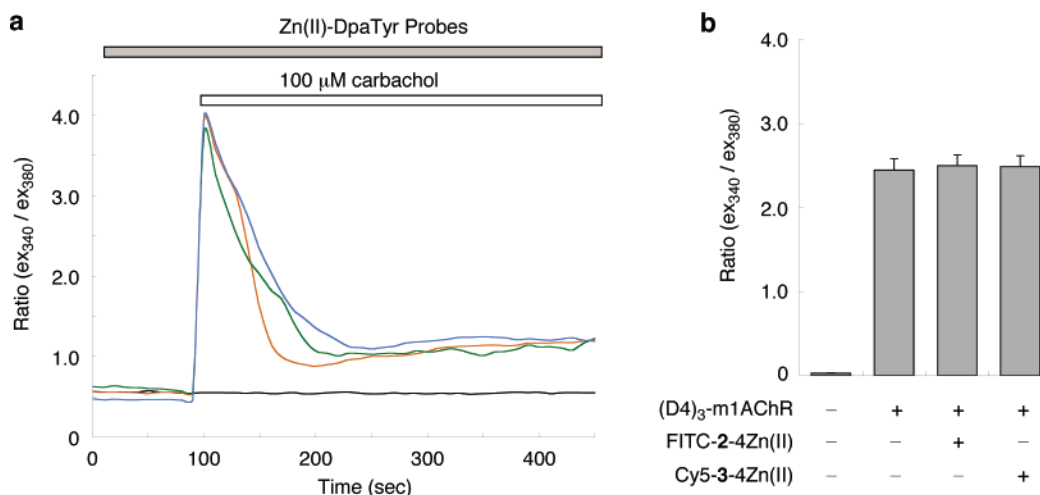


**Figure 6.** Functional analysis of labeled m1AChR with the Zn(II)-DpaTyr probes. (a) Representative time courses of  $[Ca^{2+}]_i$  response upon stimulation with 100  $\mu$ M carbachol in CHO cells expressing (D4)<sub>3</sub>-m1AChR labeled with FITC-2-4Zn(II) (green line) or Cy5-3-4Zn(II) (blue line) and unlabeled (orange line), in the presence of 2 mM extracellular  $Ca^{2+}$ . The black line shows the response of the CHO cells transfected with control vehicle vector under the same conditions. (b) Average maximum  $[Ca^{2+}]_i$  increase induced by the carbachol (100  $\mu$ M) stimulation ( $N > 30$ ).

**Synthesis of the Oligo-aspartate Peptides, Oligo-glutamate Peptides, His6 Peptide, and Tag-Fused RNases.** The oligo-aspartate or oligo-glutamate peptides were synthesized by stepwise liquid-phase condensation (EDC as a condensation reagent) and deprotection (TFA treatment) reactions using Boc-Asp(OBzl)-OH or Boc-Glu(OBzl)-OH as a condensation unit, respectively. The His6 peptide was synthesized by an automated peptide synthesizer (ABI 433A, Applied Biosystems) using standard Fmoc-based FastMoc coupling chemistry and purified by reverse-phase HPLC. The series of mutant RNases were constructed by the self-assembly of an S-protein (purchased from Aldrich) with an S-peptide tethering a D4, D4-G-D4, or His tag, which was synthesized by the automated peptide synthesizer and purified by reverse-phase

HPLC. Detailed synthetic procedures and compound characterizations are described in the Supporting Information.

**Isothermal Titration Calorimetry (ITC) Measurements.** ITC titration was performed with an isothermal titration calorimeter from MicroCal Inc. All measurements were conducted at 298 K. In ITC experiments with the oligo-aspartate, oligo-glutamate peptides, or the His6 peptide, a solution of the peptide (0.5 mM) in 50 mM HEPES buffer (pH 7.2) was injected stepwise (10  $\mu$ L  $\times$  24 times) to a solution of 1-Zn(II) (25  $\mu$ M) dissolved in the same solvent system. In the case of the RNase or the tag-fused RNase (D4-RNase, D4-G-D4-RNase, and His6-RNase), a solution of 1-2Zn(II) or 2-4Zn(II) (0.2–3 mM) in 50 mM HEPES buffer (pH 7.2) containing 100 mM NaCl was injected

stepwise ( $5\ \mu\text{L} \times 48$  times) to a solution of the RNase ( $10\text{--}50\ \mu\text{M}$ ) dissolved in the same solvent system. The measured heat flow was recorded as function of time and converted into enthalpy ( $\Delta H$ ) by integration of the appropriate reaction peaks. Dilution effects were corrected for by subtracting the result of a blank experiment with an injection of the HEPES solution into the cell in identical experimental conditions. The binding parameters ( $K_{\text{app}}$ ,  $\Delta H$ ,  $\Delta S$ ,  $n$ ) were evaluated by applying one site model using the software Origin (MicroCal Inc.).

**Circular Dichroism (CD) Measurements.** CD spectra were recorded using a JASCO J-720W spectropolarimeter. The aqueous stock solution of the Dn ( $n = 2\text{--}4$ ) peptide was titrated into the solution of 1-2Zn(II) ( $5\text{--}20\ \mu\text{M}$ ) in 50 mM HEPES buffer (pH 7.2), and the CD spectrum was measured from 200 to 400 nm (scan speed, 500 nm/min) at 25 °C using a quartz cell (1 cm path length). Each spectrum represents the average of 10 scans with smoothing to reduce noise. For the Job plot, titration of continuous variation was conducted, with the concentrations of both 1-2Zn(II) and the D4 peptide varied between 0 and 40  $\mu\text{M}$  while the number of moles in solution remained constant.

**Staining of m1AChR Receptor Tethering a (D4)<sub>3</sub> Tag on a Cell Surface.** CHO cells plated on a coverslip were placed onto a perfusion chamber filled with 0.5 mL of HEPES-buffered saline (HBS, containing 107 mM NaCl, 6 mM KCl, 1.2 mM MgSO<sub>4</sub>, 2 mM CaCl<sub>2</sub>, 11.5 mM glucose, 20 mM HEPES, adjusted to pH 7.4 with NaOH) on the stage of the microscope and stained with a 2  $\mu\text{M}$  concentration of FITC-2-4Zn(II) in HBS containing a 20  $\mu\text{M}$  concentration of the D4 peptide for 5 min. In the case of staining with Cy5-3-4Zn(II), the cells plated on a coverslip were stained with a 1  $\mu\text{M}$  concentration of Cy5-3-4Zn(II) in HBS containing a 20  $\mu\text{M}$  concentration of the D4 peptide for 7 min. The coverslip was washed once with HBS buffer to remove excess probe, and the chamber was filled with 0.5 mL of HBS for fluorescence imaging. Fluorescence images of the cells were recorded using a

FLUOVIEW confocal laser-scanning microscope (OLYMPUS) equipped with the appropriate excitation and emission filters for fluorescein, Cy5, EGFP, and DsRed.

**Measurement of the Intracellular Ca<sup>2+</sup> Concentration ([Ca<sup>2+</sup>]<sub>i</sub>).** The fura-2 fluorescence images of the cells were recorded and analyzed as described previously.<sup>18</sup> Briefly, CHO cells on coverslips were loaded with fura-2 by incubation in F12 containing 10  $\mu\text{M}$  fura-2/AM (Dojindo) and 10% fetal bovine serum at 37 °C for 20 min. The cells were washed once with HBS (containing a 2 mM concentration of CaCl<sub>2</sub>) and stained with a 1  $\mu\text{M}$  concentration of the Zn(II)-DpaTyr probes (if necessary). The coverslips were then plated on a perfusion chamber mounted on the stage of the microscope, and fluorescence images were recorded and analyzed with a video image analysis system (Aqua Cosmos, Hamamatsu Photonics) upon stimulation with 100  $\mu\text{M}$  carbachol in HBS. Fluorescence at the emission wavelength of 510 nm was measured at room temperature by exciting fura-2 alternately at 340 and 380 nm. The 340:380 nm ratio images were obtained on a pixel-by-pixel basis.

**Supporting Information Available:** Detailed synthetic procedures and compound characterizations, CD titration, fluorescence labeling and functional analysis of the tag fused receptor protein, evaluation of cell toxicity, and plasmid constructions. This material is available free of charge via the Internet at <http://pubs.acs.org>.

JA0618604

- (18) (a) Nishida, M.; Sugimoto, K.; Hara, Y.; Mori, E.; Morii, T.; Kurosaki, T.; Mori, Y. *EMBO J.* **2003**, *22*, 4677. (b) Hara, Y.; Wakamori, M.; Ishii, M.; Maeno, E.; Nishida, M.; Yoshida, T.; Yamada, H.; Shimizu, S.; Mori, E.; Kudoh, J.; Shimizu, N.; Kurose, H.; Okada, Y.; Imoto, K.; Mori, Y. *Mol. Cell* **2002**, *9*, 163.